A MULTISCALE FINITE-VOLUME METHOD FOR THREE-PHASE FLOW INFLUENCED BY GRAVITY

IVAN LUNATI AND PATRICK JENNY

Institute of Fluid Dynamics, ETH Zurich, 8092 Zurich, Switzerland

Abstract

The Multiscale Finite-Volume (MSFV) method has been developed to solve multiphase flow problems on large and highly heterogeneous domains efficiently. It employes an auxiliary coarse grid, together with its dual, to define and solve a coarse-scale pressure problem. A set of basis functions, which are local solutions on dual cells, is used to interpolate the coarse-grid pressure and obtain the approximate fine-scale pressure distribution. However, if flow takes place in presence of gravity, the basis functions are not good interpolators and a correction function, added to the basis-function interpolated pressure, is needed to obtain accurate fine-scale approximations. Numerical experiments demonstrate excellent agreement between the MSFV solutions for pressure and saturation and the corresponding fine-scale reference solutions.

1. Introduction

To model flow and transport in geological porous media efficiently, a number of upscaling techniques have been developed in the past 30 years to coarsen the numerical grid used for the simulations. The price paid to reduce the computational costs is the loss of fine-scale information. To overcome this drawback, several multiscale methods have been recently proposed to model aquifers and reservoirs: the Multiscale Finite-Element Method (Hou and Wu 1997); the Mixed Multiscale Finite-Element Method (Aarnes et al. 2005; Arbogast 2002; Chen and Hou 2003); and the Multiscale Finite-Volume (Jenny et al. 2003). In contrast to upscaling, the focus is not simply on capturing the large-scale behavior of the system, but on solving the problem with the original resolution. The goal is to be as accurate as the fine-scale solution keeping the computational costs low - ideally comparable with traditional upscaling methods.

These methods usually deal with simplified physics (incompressible flow, negligible capillary and gravity effects). Here we show the application of a multiscale algorithm to gravity-driven multiphase flow. We consider the Multiscale Finite-Volume (MSFV) method, which in contrast to other methods is based on a finite-volume discretization. This has technical and practical advantages. Indeed, a conservative flux field is obtained by solving a mass balance equation, which facilitates incorporating complex physical processes into the model. Moreover, it follows the main-stream of the currently established simulators in reservoir engineering, which are based on finite-volume discretization. These facts increase the appeal of the method for industrial and practical applications.

The MSFV method was developed to solve elliptic (homogeneous) equations on large and highly heterogeneous domains efficiently (Jenny et al. 2003) and has been applied for incompressible multiphase flow problems with negligible capillary pressure and gravity (Jenny et al. 2004). Recently, the MSFV method has been modified to incorporate additional physics and it has been applied for compressible flow (Lunati and Jenny 2006a). The modified algorithm consists of three main steps: computation of an approximate pressure solution, which includes the computation of the basis functions to extract coarse-scale effective transmissibilities and the solution of the coarse-scale pressure equation; construction of conservative fine-scale fluxes; and solution of the transport equations. In this paper we show that the pressure approximation has to be modified in order to treat flow in presence of gravity correctly.

2. Mathematical model of multiphase flow

If we consider the flow of three incompressible phases in a rigid porous medium with constant porosity, the mass balance equation of each phase $\alpha = 1, 2, 3$ is

$$\phi \frac{\partial}{\partial t} S_\alpha + \nabla \cdot \boldsymbol{u}_\alpha + q_\alpha = 0, \tag{1}$$

where ϕ $[L^3/L^3]$ is the porosity of the medium; S_α $[L^3/L^3]$ the saturation; and q_α $[1/T]$ the source term (positive when extracted). If we neglect capillary pressure and consider an isotropic porous medium, the volumetric flux per unit area, $\boldsymbol{u}_\alpha$ $[L/T]$, is given by the generalized Darcy's law, i.e.,

$$\boldsymbol{u}_\alpha = -\lambda_\alpha k \left(\nabla p - \rho_\alpha \boldsymbol{g} \right), \tag{2}$$

where λ_α is the α-phase relative mobility; k $[L^2]$ the intrinsic permeability, which is fluid independent; p $[M/LT^2]$ the pressure; ρ_α $[M/L^3]$ the density; and $\boldsymbol{g}$ $[L/T^2]$ the gravity acceleration vector.

Summing up Eqs. (1), defining the total velocity, $\boldsymbol{u} = \sum_\alpha \boldsymbol{u}_\alpha$, and the total source term, $q = \sum_\alpha q_\alpha$, and noting that $\sum_\alpha S_\alpha = 1$, we obtain

$$\nabla \cdot \boldsymbol{u} + q = 0. \tag{3}$$

According to Eq. (2), the total velocity can be written as

$$\boldsymbol{u} = -\lambda k \left(\nabla p - \boldsymbol{G} \right), \tag{4}$$

where

$$\boldsymbol{G} = \boldsymbol{g} \sum_\alpha f_\alpha \rho_\alpha, \tag{5}$$

$[M/T^2L^2]$, is the modified gravity; $\lambda = \sum_\alpha \lambda_\alpha$ the total mobility; and $f_\alpha = \lambda_\alpha/\lambda$ the fractional flow function of the α-phase. Once Eq. (3) has been solved for the pressure, p, the velocities of two phases can be computed and used in the two corresponding transport equations, which have the form of Eq. (1). The saturation of the third phase can be obtained from the constraint $\sum_\alpha S_\alpha = 1$.

3. Finite-volume discretization

Given a grid with M nodes and N cells, which defines a partition of the domain, Ω, into N control volumes, $\Omega_{i\in[1,N]}$, we can derive a set of discrete mass-balance equation by integrating Eq. (3) over each control volume, i.e., $\int_{\Omega_i}\left\{\nabla\cdot\boldsymbol{u}+q\right\}\,d\boldsymbol{x}=0$. Neglecting the source term, using Eq. (4), and applying Gauss' theorem (or divergence theorem), we can write

$$\sum_j\int_{\partial\Omega_{ij}}\lambda k\nabla p\cdot\boldsymbol{\eta}\;d\Gamma=\sum_j\int_{\partial\Omega_{ij}}\lambda k\;\boldsymbol{G}\cdot\boldsymbol{\eta}\;d\Gamma, \tag{6}$$

where $\partial\Omega_{ij}=\partial\Omega_i\cap\partial\Omega_j$ is the interface between two cells, Ω_i and Ω_j, $\boldsymbol{\eta}$ the unit vector orthogonal to $\partial\Omega_{ij}$ pointing from Ω_i to Ω_j. In Eq. (6) a choice has to be made in order to relate the continuous pressure gradient, ∇p, to the discrete potential drop between the two cells, p_i-p_j. In the standard cell-centered finite-volume scheme, a piecewise linear interpolation is used and flux continuity is enforced at the interface; in the MSFV method localized fine-scale solutions of the pressure equation are used as pressure interpolators.

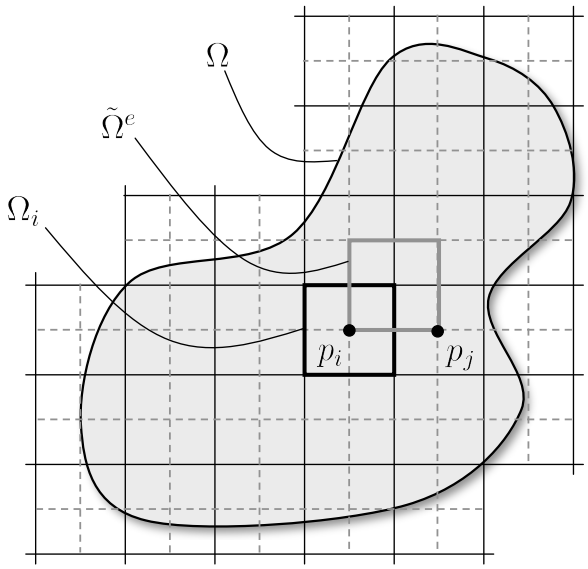

Figure 1. The coarse grid (solid line) together with its dual (dashed line)

.

4. The Multiscale Finite-Volume Method

In the MSFV method an auxiliary coarse grid with M nodes and N cells is constructed, which defines a partition, $\Omega_{i\in[1,N]}$, of the domain Ω. A dual coarse grid is constructed such that each dual coarse cell, $\tilde{\Omega}^{e\in[1,M]}$, contains exactly one node of the coarse grid in its interior. The dual coarse grid has N nodes, $\boldsymbol{x}_{j\in[1,N]}$, exactly one in the interior of each coarse cell (Fig. 1).

The modified MSFV method, (Lunati and Jenny 2006a), consists of three main steps: computation of an approximate pressure field, which includes the solution of a coarse-scale pressure equation; construction of conservative fine-scale fluxes; and solution of the phase-transport equations. The pressure approximation consists of a juxtaposition of local solutions computed on the dual cells. To compute the fine-scale pressure approximation, a set of basis functions and a correction function are employed. The basis functions, which are local solutions of the elliptic homogeneous equation, are used to relate the coarse-grid pressure to the fine-scale pressure distribution and to extract the coarse-scale transmissibilities. The correction function, which is independent of the coarse-scale pressure, is used to account for the gravity effects and correct the coarse-scale operator.

Once the approximate pressure is obtained, the fluxes induced at the coarse-cell boundaries are extracted and used as Neumann boundary conditions for local problems (one in each coarse cell) which are solved to compute a conservative fine-scale flow field. Therefore, the flux approximation is defined as a juxtaposition of local solutions computed on the coarse cells. Mass conservation is guaranteed by the fact that fluxes are continuous at the coarse-cell interfaces since adjacent cells share the same flux boundary conditions (with opposite sign).

The conservative total-flux field is used in the phase-transport equations, which are solved by a Schwatz's overlapping method using an implicit scheme locally within the coarse cells. Since mobility depends on saturation, basis functions have to be updated. In order to keep the MSFV method efficient it is crucial that the basis functions are update adaptively only in regions where mobility changes exceed a given threshold. Like this, most functions can be reused for the successive step. In the following, we describe how the pressure approximation is constructed and refer to (Lunati and Jenny 2006a; Lunati and Jenny 2006b) for a more comprehensive description of the method including the adaptivity criterion to update the basis and correction functions; the construction of the flux approximation; the solution of the phase transport equations; and the coupling between pressure and saturation equations.

4.1. **Fine-scale pressure approximation.** The MSFV method relies on approximating the fine-scale pressure by a juxtaposition of localized solutions computed in the dual cells, $p|_{\tilde{\Omega}^e}$, and on the representation of these solutions as

$$p|_{\tilde{\Omega}^e} = \sum_j \tilde{\varphi}^e_j p_j + \tilde{\varphi}^e_*, \tag{7}$$

where the basis functions, $\tilde{\varphi}^e_j$, are local solutions of

$$\begin{cases} \nabla \cdot \lambda k \nabla \tilde{\varphi}^e_j = 0 & \text{on} \quad \tilde{\Omega}^e \\ \nabla_\perp \cdot \lambda k \nabla \tilde{\varphi}^e_j = 0 & \text{on} \quad \partial\tilde{\Omega}^e \\ \tilde{\varphi}^e_j(\boldsymbol{x}_i) = \delta_{ij} \end{cases}, \tag{8}$$

and the correction function, $\tilde{\varphi}^e_*$ of

$$\begin{cases} \nabla \cdot \lambda k \left(\nabla \tilde{\varphi}^e_* - \boldsymbol{G}\right) = 0 & \text{on} \quad \tilde{\Omega}^e \\ \nabla_\perp \cdot \lambda k \left(\nabla \tilde{\varphi}^e_* - \boldsymbol{G}\right) = 0 & \text{on} \quad \partial\tilde{\Omega}^e \\ \tilde{\varphi}^e_*(\mathbf{x}_i) = 0 \end{cases}. \tag{9}$$

Note that the boundary condition assigned on $\partial\tilde{\Omega}^e$ is equivalent to require that

$$\nabla_\perp \cdot \boldsymbol{u} = 0 \quad \text{on} \quad \partial\tilde{\Omega}^e, \tag{10}$$

where the subscript $_\perp$ denotes the vector component perpendicular to $\partial\tilde{\Omega}^e$, and

$$p(\boldsymbol{x}_j) = p_j. \tag{11}$$

This boundary condition proved to provide accurate results for a large set of numerical test cases (Jenny et al. 2003; Jenny et al. 2004; Lunati and Jenny 2006a). Since the velocity is divergence free and $\nabla \cdot \boldsymbol{u} = \nabla_\perp \cdot \boldsymbol{u} + \nabla_\parallel \cdot \boldsymbol{u}$, Eq. (10) is equivalent to assign the solution of the reduce problem $\nabla_\parallel \cdot \boldsymbol{u} = 0$ as Dirichlet boundary conditions on $\partial\tilde{\Omega}^e$, where the subscript $_\parallel$ denotes the vector component parallel to $\partial\tilde{\Omega}^e$.

4.2. **Coarse-scale problem.** The coarse-scale pressure equation can be obtained inserting the approximate pressure, Eq. (7), into Eq. (6). This yields the following set of discrete coarse-cell mass-balance equations:

$$\sum_j T_{ij} p_j = \sum_e \int_{\partial\Omega_i \cap \tilde{\Omega}^e} \lambda k \nabla \tilde{\varphi}^e_* \cdot \boldsymbol{\eta} \, ds - \int_{\partial\Omega_i} \lambda k \, \boldsymbol{G} \cdot \boldsymbol{\eta} \, ds \quad i \in [1, N], \tag{12}$$

where the transmissibilities,

$$T_{ij} = -\sum_e \int_{\partial\Omega_i \cap \tilde{\Omega}^e} \lambda k \nabla \tilde{\varphi}^e_j \cdot \boldsymbol{\eta} \, ds, \tag{13}$$

are defined as in the case without gravity effects. The terms on the r.h.s. of Eq. (12) represent two surface source terms on $\partial\Omega_i$. Since the coarse-scale operator, T_{ij}, does not include gravity effects, it yields fluxes across $\partial\Omega_i$ that are incorrect. The first term on the r.h.s. of Eq. (12) represents a correction to these inaccurate fluxes and can be regarded as a local correction to the coarse-scale operator, T_{ij}, independent of the coarse-scale pressure.

5. Numerical tests

In this section the accuracy of the MSFV method for density-driven flow is investigated by comparison with a fine-scale reference solution. We consider a 1D counter-current flow problem in a homogeneous permeability field and a 2D lock-exchange problem in a heterogeneous permeability field. In both cases no-flow conditions apply to all boundaries.

	$\mu_\alpha[Pa\ s]$	$\rho_\alpha[kg/m^3]$
water	10^{-3}	1000
brine	10^{-3}	1100
heavy oil	10^{-2}	900
light oil	10^{-2}	500

Table 1. Properties of the phases used for the numerical simulations

5.1. **Counter-current flow.** We consider a three-phase counter-current flow in an homogeneous permeability field. Initially, the lower part of the domain is filled with 50% heavy oil and 50% brine, and the upper part with 100% water. Quadratic mobilities are assumed for all phases; phase viscosities and densities are given in Tab.1. At time zero brine and oil begin to separate due to buoyancy effects. When the brine saturation decreases at the water interface, the water becomes heavier than the "mixture" below and starts moving downwards, while oil continues flowing upwards. This numerical experiment allows to have in a single test a stable interface (water/brine), an unstable interface (water/oil), and phase separation.

The numerical solutions are computed on a 1D domain of size L, which is discretized into 54 fine cells. The coarse grid used for the MSFV method consists of 9 cells. In Fig. 2, the evolution of the vertical profiles of oil and water saturation obtained with the MSFV method are compared with the corresponding fine-scale reference solutions. It can be observed that solutions are almost identical.

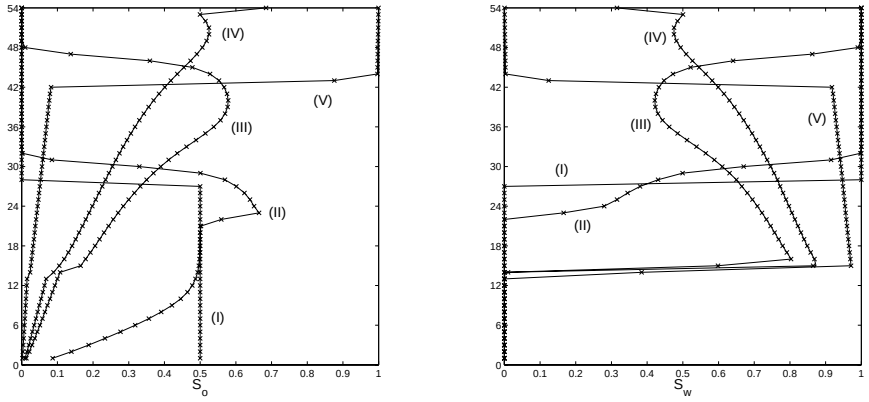

(a) (b)

FIGURE 2. Counter-current flow. Vertical profiles of oil-phase (a) and water-phase saturation (b) at different times, (I)-(V). Fine-scale solution (solid lines) and MSFV solution (crosses).

5.2. **Lock-exchange problem.** We consider a three-phase system consisting of water, light oil and a dummy phase, which has the same properties of the the oil phase. Initially, water occupies the left half of the domain, while the right part is filled with oil. Due to the density difference, recirculation is induced. Here, in contrast to the counter-current flow problem, gravity significantly contributes to the total velocity and therefore an accurate global pressure information is needed to correctly capture the flow induced in the horizontal direction. The saturation of the dummy phase, which is initially not present in the system, is obtained from the constraint $\sum_\alpha S_\alpha = 1$ and is used to check material-balance: the error has to remain smaller than the specified saturation-error tolerance. Quadratic mobilities are assumed for all phases; phase viscosities and densities are given in Tab.1.

The numerical solutions are computed on a 2D domain of size $L \times L$, which is discretized into 54×54 fine cells. The coarse grid used for the MSFV method consists of 9×9 cells. The geometric mean of the heterogeneous permeability field (Fig. 3.d) is $k_g = 1.3\ 10^{-9} m^2$

and the variance of the log-normal permeability is $\sigma^2_{\ln k} = 2.52$. In Fig. 3, the evolution of the saturation distribution obtained with the MSFV method is compared with the fine-scale reference solutions. Shown are water-saturation contour lines at three different times. Note the sharp drainage front (oil invasion) and the expansion wave behind the wetting front (water invasion) due to viscosity difference. The two solutions are in excellent agreement even after large simulation times, which proves that the velocities of the two invading fronts are accurately captured by the MSFV method. The saturation of the dummy phase always remains smaller that the error tolerance of the phase-transport equations.

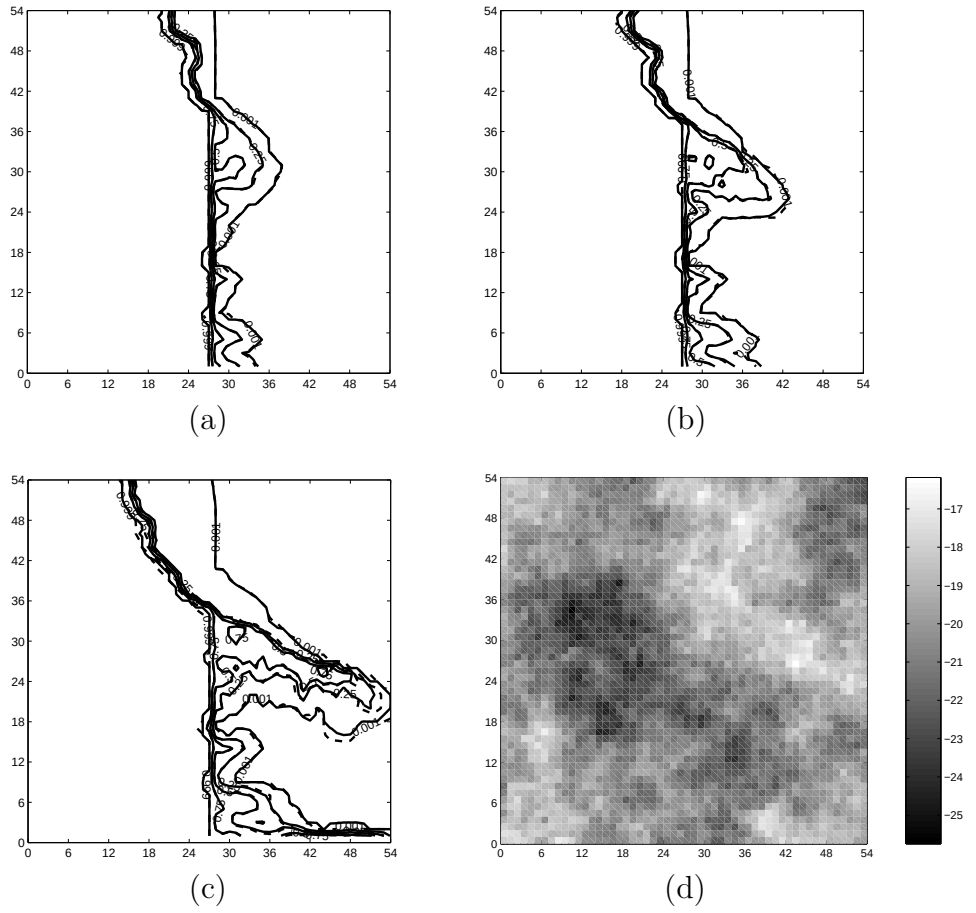

FIGURE 3. Lock exchange problem. (a)-(c) Water-phase saturation contour lines (0.001, 0.25, 0.5, 0.75, 0.999) at three different times. Fine-scale solution (solid contours) and MSFV solution (dashed contours). (d) The natural logarithm of the heterogeneous permeability field; the geometric mean of the permeability field is $k_g = 1.3\ 10^{-9} m^2$; the variance of the log-permeability is $\sigma^2_{\ln k} = 2.52$

6. Conclusions

An accurate treatment of density-driven flow in the MSFV method has been achieved adding a correction function to the basis-function interpolated pressure. This correction yields very accurate fine-scale pressure fields. The numerical experiments performed for density-driven flow problems (counter-current flow and lock-exchange) demonstrate that the MSFV solutions for pressure and saturation are in excellent agreement with the corresponding fine-scale reference solutions.

References

Aarnes, J., V. Kippe, and K. Lie (2005). Mixed multiscale finite elements and streamline methods for reservoir simulation of large geomodel. *Adv. Water Res. 28*, 257–271.

Arbogast, T. (2002). Implementation of a locally conservative numerical subgrid upscaling scheme for two phase darcy flow. *Computational Geosciences 6*, 453–481.

Chen, Z. and T. Y. Hou (2003). A mixed finite element method for elliptic problems with rapidly oscillating coefficients. *Math. Comput.*.

Hou, T. Y. and X. H. Wu (1997). A multiscale finite element method for elliptic problems in composite materials and porous media. *J. Comp. Phys 134*(1), 169–189.

Jenny, P., S. H. Lee, and H. Tchelepi (2003). Multi-scale finite-volume method for elliptic problems in subsurface flow simulation. *J. Comp. Phys 187*(1), 47–67.

Jenny, P., S. H. Lee, and H. Tchelepi (2004). Adaptive multiscale finite-volume method for multi-phase flow and transport in porous media. *Multiscale Model. Simul. 3*(1), 50–64.

Lunati, I. and P. Jenny (2006a). Multi-scale finite-volume method for compressible flow in porous media. *J. Comp. Phys*. In Press, Available online 10 February 2006, doi:10.1016/j.jcp.2006.01.001.

Lunati, I. and P. Jenny (2006b). Multiscale finite-volume method for density driven flow in porous media. *Comput. Geosci.*. Submitted.

I. Lunati, Institute of Fluid Dynamics, ETH Zurich, 8092 Zurich, Switzerland
E-mail address: lunati@ifd.mavt.ethz.ch